

# PHOTONICS Research

## 1.7- $\mu\text{m}$ dissipative soliton Tm-doped fiber laser

Ji-Xiang Chen,<sup>1</sup> Xiang-Yue Li,<sup>1</sup> Ti-Jian Li,<sup>1</sup> Ze-Yu Zhan,<sup>1</sup> Meng Liu,<sup>1</sup> Can Li,<sup>2</sup> Ai-Ping Luo,<sup>1</sup> Pu Zhou,<sup>2</sup> Kenneth K.-Y. Wong,<sup>3</sup> Wen-Cheng Xu,<sup>1,4</sup> and Zhi-Chao Luo<sup>1,\*</sup>

<sup>1</sup>Guangdong Provincial Key Laboratory of Nanophotonic Functional Materials and Devices & Guangzhou Key Laboratory for Special Fiber Photonic Devices and Applications, South China Normal University, Guangzhou 510006, China

<sup>2</sup>College of Advanced Interdisciplinary Studies, National University of Defense Technology, Changsha 410073, China

<sup>3</sup>Department of Electrical and Electronic Engineering, The University of Hong Kong, Hong Kong, China

<sup>4</sup>e-mail: xuwch@scnu.edu.cn

\*Corresponding author: zcluo@scnu.edu.cn

Received 7 January 2021; revised 8 March 2021; accepted 9 March 2021; posted 9 March 2021 (Doc. ID 419273); published 30 April 2021

We report on the dissipative soliton generation in a 1.7- $\mu\text{m}$  net-normal dispersion Tm-doped fiber laser by non-linear polarization rotation technique. An intra-cavity bandpass filter was employed to suppress the long-wavelength emission, while the cavity dispersion was compensated by a segment of ultrahigh numerical aperture (UHNA4) fiber. The dissipative soliton with a central wavelength of 1746 nm was obtained, covering a spectral range from 1737 nm to 1754 nm. The de-chirped duration and energy of the dissipative soliton were 370 fs and 0.2 nJ, respectively. In addition, the dynamics of multiple dissipative solitons were also investigated. Through optimization of the cavity dispersion, the 50 nm broadband dissipative soliton with de-chirped pulse duration of 230 fs could be achieved. The development of dissipative soliton seed laser represents the first step in achieving the chirped pulse amplification system at the 1.7- $\mu\text{m}$  wave band, which would find potential applications in fields such as biomedical imaging and material processing.

© 2021 Chinese Laser Press

<https://doi.org/10.1364/PRJ.419273>

### 1. INTRODUCTION

Ultrafast fiber lasers represent an important tool in the two-way interface investigations of fundamental nonlinear optics and laser engineering, covering a wide range of scientific and technical fields [1]. With the rapid progress of fiber fabrication and laser technology, the investigations of ultrafast fiber lasers have been greatly stimulated in recent decades. So far, ultrafast fiber lasers have been applied to diverse fields such as laser micromachining [2], biomedicine [3], and optical communications [4]. In fact, the operation wave band of a fiber laser is critical to practical applications. Therefore, the development of fiber lasers at desirable wave band is strongly motivated by specific applications. Recent advances show that the 1.7- $\mu\text{m}$  ultrafast fiber lasers could find important applications in biomedical imaging and spectroscopic analysis [5–7], owing to the deeper tissue penetration and abundant molecular absorption in this spectral wave band. Thus, developing high-performance 1.7- $\mu\text{m}$  ultrafast fiber lasers could enable high-resolution biomedical imaging with deeper penetration depth and the spectroscopy of biological materials containing specific bonds.

The great demand for 1.7- $\mu\text{m}$  ultrafast fiber lasers has driven laser scientists to focus on efficient solutions to realize the ultrashort pulse in this wave band. In fact, owing to the lack of the effective gain medium, first the nonlinear frequency conversion, namely soliton self-frequency shift, was proposed to

generate the ultrashort pulse at the 1.7- $\mu\text{m}$  wave band [8,9]. However, the amount of frequency shift is dependent on the pulse peak power, resulting in the contradiction between the output pulse energy and the targeted wave band. Moreover, the temporal coherence of soliton might also degenerate during the conversion process, which will lead to the wave breaking of the input soliton. In addition to nonlinearly converted lasers, the 1.7- $\mu\text{m}$  pulse can be directly generated with a proper gain fiber. A new gain medium bismuth-doped fiber [10] has been demonstrated to enable the 1.7- $\mu\text{m}$  laser operation. Nevertheless, the currently reported bismuth-doped fiber is still in the early stages of research and is not commercially available. In fact, from the viewpoint of practical applications, the commercially available gain medium would be preferred.

Recently, the commercial thulium-doped fiber (TDF), with its broad emission spanning from 1600 nm to 2100 nm in the  $^3\text{F}_4 - ^3\text{H}_6$  transition [11,12], has been proved to be an alternative way to produce effective optical gain in the 1.7- $\mu\text{m}$  wave band [13,14]. However, due to the largely anomalous dispersion in silica-based TDF and single-mode fiber (SMF), to date the mode-locking of 1.7- $\mu\text{m}$  fiber lasers generally operated in the conventional soliton regime [15–18]. In this case, the wave breaking of conventional solitons owing to the overdriven nonlinear effect in optical fiber limits the achievable pulse energy [19]. Actually, for most applications such as brain imaging and medical surgery, the high-energy pulse is desirable.

Thus, there is a strong motivation to develop the 1.7- $\mu\text{m}$  high-energy pulse fiber laser systems. Nowadays, the pulse energy directly emitted from the fiber lasers could be greatly enhanced by skillfully engineering the cavity dispersion to normal/net-normal ones, which refers to dissipative solitons [20,21]. In addition, dissipative solitons are beneficial for further amplification by subsequent chirped-pulse amplification (CPA) systems as a seeding source [22–24]. Therefore, a question naturally arises as to whether the dissipative soliton can be realized in a 1.7- $\mu\text{m}$  thulium-doped fiber laser through the dispersion engineering approach.

In this work, we report on the dissipative soliton generation in a net-normal dispersion mode-locked Tm-doped fiber laser operating at the 1.7- $\mu\text{m}$  wave band. The mode-locking was realized via the nonlinear polarization rotation (NPR) technique, and the cavity dispersion was controlled by adjusting the length of the ultrahigh numerical aperture (UHNA4) fiber [25,26]. The mode-locked spectrum shows a rectangular profile, which is the typical feature of dissipative soliton. The de-chirped pulse duration could reach 230 fs when the cavity dispersion was optimized. Additionally, the multi-soliton patterns were also discussed. It is believed that the results would be meaningful for obtaining the high-energy pulse from the fiber laser systems at the 1.7- $\mu\text{m}$  wave band.

## 2. EXPERIMENTAL SETUP

The schematic of the Tm-doped mode-locked fiber laser is shown in Fig. 1. A 3.3-m long single-mode Tm-doped fiber (SM-TSF-9/125, Nufern) served as the gain medium, which was core-pumped by an erbium-doped fiber amplifier operating at 1560 nm. The polarization-dependent isolator ensures the unidirectional operation and provides polarization selectivity. An in-line polarization controller (PC) is included to adjust the polarization state of the propagation light. A 20/80 optical coupler with the 80% port guiding the laser output. At the 1.7- $\mu\text{m}$  wave band, silica-based thulium-doped fiber requires large population inversion to achieve short-wavelength gain due to the quasi-three-level nature. Large population inversion leads to amplified spontaneous emission (ASE) at long wavelengths. Thus, a bandpass filter (BPF) with a center wavelength of 1740 nm and a bandwidth of 25 nm was inserted between two collimators to suppress ASE at the long wavelength and stabilize the dissipative soliton operation [27]. The BPF we used is an interference filter, which has a maximum transmittance of 75%. The net cavity dispersion was compensated by

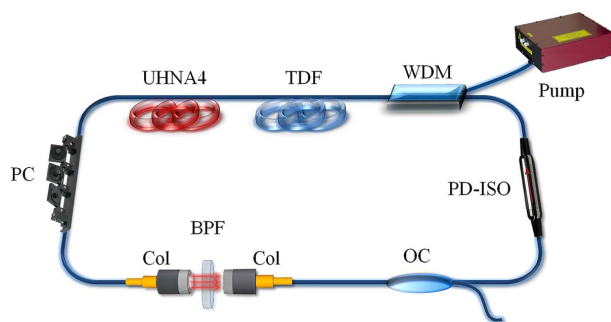


**Fig. 1.** Schematic of the dissipative soliton Tm-doped fiber laser.

**Table 1.** Fiber Dispersion Values

Fiber Type	SMF – 28e	TDF	UHNA4
GVD ( $\text{ps}^2/\text{m}$ )	–0.045	–0.045	0.085
Length (m)	2.3	3.2	6
GDD ( $\text{ps}^2$ )	–0.104	–0.144	0.510

using a segment of UHNA4 fiber (Nufern). The cavity length is about 11.5 m, corresponding to the 17.84 MHz fundamental repetition rate. The length, group velocity dispersion (GVD), and group delay dispersion (GDD) of TDF, SMF, and UHNA4 fibers are listed in Table 1. The dispersion values are given for the central wavelength of 1750 nm [28]. Note that the pigtailed of all optical devices are SMF – 28e. Thus, the total net cavity dispersion is about 0.26  $\text{ps}^2$ , showing that the laser operates in the net-normal dispersion region. The laser spectrum and the mode-locked pulse were measured by a spectral analyzer (Yokogawa, AQ6375B) and an oscilloscope (Tektronix, DSA71604B, 16 GHz) with a photodetector (New Focus P818-BB-35F, 12.5 GHz). Moreover, a commercial autocorrelator (Femtochrome, FR-103WS) was used to measure the pulse duration.

## 3. EXPERIMENTAL RESULTS

As we know, the NPR-based saturable absorption effect is related to the polarization state and pump power level [29]. Therefore, with the proper rotation of the PC, the single-pulse operation could be obtained at a pump power of 1.04 W. Figure 2 shows the typical mode-locked operation with the fundamental repetition rate at the 1.7- $\mu\text{m}$  wave band. As illustrated in Fig. 2(a), the mode-locked spectrum shows a quasi-rectangular profile with steep spectral edges on both sides under the logarithmic coordinates, which are the typical characteristics of dissipative soliton. For better clarity, the linear coordinate of the mode-locked spectrum is also plotted with a blue dotted curve in Fig. 2(a). The central wavelength locates at 1746 nm, and the spectral width at 10 dB is about 17 nm. Note that the central wavelength can be slightly tuned by rotating the PC owing to the Lyot filtering effect in NPR mode-locked fiber lasers [30]. Figure 2(b) presents the mode-locked pulse train. The pulse repetition rate, which is determined by the cavity length, is 17.84 MHz. Correspondingly, the output power is 3.55 mW, indicating that the pulse energy of  $\sim 0.2$  nJ is obtained. Moreover, the measured pulse train in a large temporal range is also presented in the inset of Fig. 2(b). The pulse duration was measured to be 3.9 ps, as shown in Fig. 2(c). Due to the net-normal dispersion of the laser cavity, the output dissipative solitons are chirped directly outside the cavity, which can be further compressed if the dispersion compensation component is employed. We recall that the conventional SMF can be used as pulse compressor at the 1.7- $\mu\text{m}$  wave band, provided that the dissipative soliton is generated from a normal or net-normal dispersion fiber laser. Therefore, the dissipative soliton was injected into a 25-m long SMF for pulse compression. After de-chirping, the autocorrelation trace of the mode-locked pulse is plotted with the red curve in Fig. 2(c). If the Gaussian profile is assumed, the pulse duration after compression is  $\sim 370$  fs. Figure 2(d) shows the radio frequency

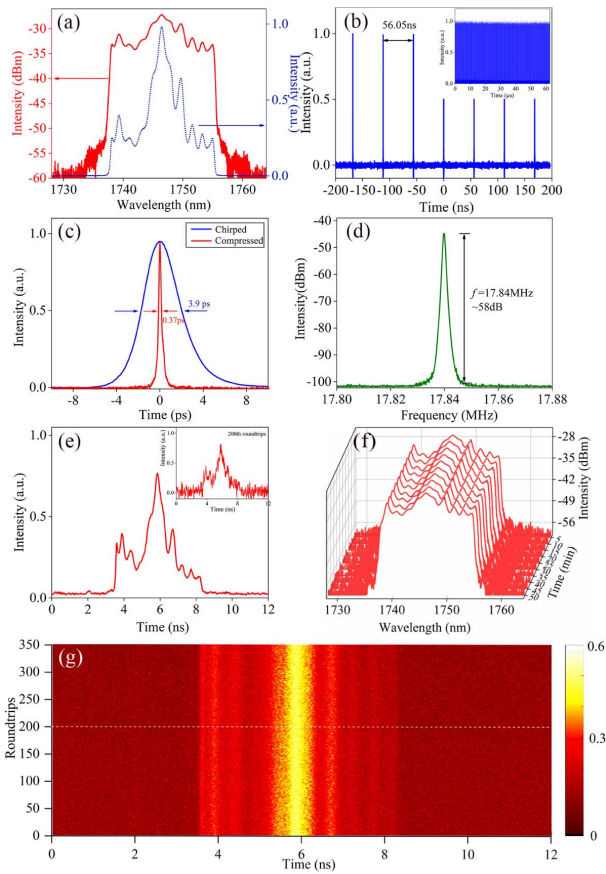


**Fig. 2.** Single-pulse operation. (a) Mode-locked spectrum; (b) pulse train, inset: pulse train over 60  $\mu$ s; (c) the measured autocorrelation trace of the uncompressed output pulse (blue) and the compressed pulse (red); (d) RF spectrum; (e) averaged shot-to-shot spectrum, inset: single-shot spectrum of the 200th round trip; (f) shot-to-shot spectrum with 350 round trips; (g) real-time spectral evolution by DFT.

(RF) spectrum of the mode-locked dissipative soliton with a resolution bandwidth of 1 kHz. As can be seen here, the frequency peak locates at 17.84 MHz, which corresponds to the fundamental repetition rate. In addition, the signal-to-noise ratio is about 58 dB, demonstrating that the proposed fiber laser was operating in the stable single-pulse regime.

To further investigate the characteristics of the single-pulse operation in detail, the dispersive Fourier transform (DFT) technique was used to capture the real-time spectral dynamics on the oscilloscope based on frequency to time mapping [31,32]. Here, owing to the acceptable loss of SMF-28e at the 1.7- $\mu$ m wave band, the DFT was realized by injecting the mode-locked pulse into a 10 km SMF-28e. Therefore, the single-shot spectral profile of the dissipative soliton can be resolved by the DFT. As depicted in Fig. 2(g), the intensities and the shot-to-shot spectral profiles are nearly the same as each other along the cavity round trips. Thus, no instantaneous instability could be observed for the single-pulse regime. Apart from that, the averaged shot-to-shot spectra as well as the single-shot spectrum of the 200th round trip are plotted in Fig. 2(e). Here, the spectral profile measured by DFT is in agreement with the optical spectrum analyzer (OSA) recorded

spectrum, confirming that no spectral information was lost during the DFT process. In order to check the long-term stability of the 1.7- $\mu$ m dissipative soliton fiber laser, we repeatedly scanned the output spectrum at 5-min intervals over 50 min. The results are plotted in Fig. 2(f). There is no obvious intensity fluctuation or wavelength drift on the mode-locked spectrum, which further verifies the stability of the proposed 1.7- $\mu$ m ultrafast fiber laser.

It has been well known that the pulse splitting effect owing to the overdriven nonlinear phase shift could be induced in a mode-locked fiber laser, if the pump power is high enough [33]. In this case, the fiber laser would step into the multi-soliton regime with more complex behavior. Thus, as the pump power was increased to  $\sim 1.15$  W, the dissipative soliton was splitting into the double-soliton regime, as shown in Fig. 3(b). However, owing to the slight increase of the pump power, the mode-locked spectrum is similar to that of the single-soliton one, which is plotted in Fig. 3(a). In fact, the mode-locked spectrum measured by the OSA is the superposition of two solitons. Therefore, the spectrum of individual soliton cannot be identified. Note that the temporal interval of the two solitons is about 21 ns. Thus, it is possible to record the individual real-time spectrum of two solitons by using the DFT technique [34,35]. Figure 3(c) shows the shot-to-shot DFT spectra of two solitons with 350 round trips. It can be seen that the spectral profiles of the two solitons are almost identical, and the interval between them remains stable during propagation. In addition, we also provided the averaged shot-to-shot spectra of two solitons in Fig. 3(c), which shows the same spectral profile as each other. The above results confirm that the two solitons possess the same temporal and spectral features.

By slightly adjusting the orientation of the PC, the output power and polarization states of two dissipative solitons shown in Fig. 3 will change. In this case, the phase delay between the two solitons might vary as well. Thus, it is possible to tune the interval of two solitons by rotating the PC. Correspondingly, the two solitons moved close to each other and eventually became indistinguishable on the oscilloscope trace, as presented in Fig. 4(b). Under this condition, it is evident that the periodic

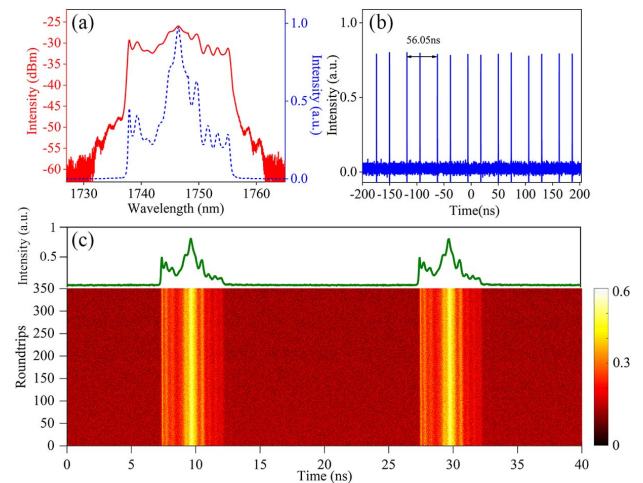


**Fig. 3.** Double pulse operation. (a) Spectrum with log and linear coordinates; (b) pulse train; (c) shot-to-shot spectrum over 350 round trips, inset: averaged shot-to-shot spectrum.

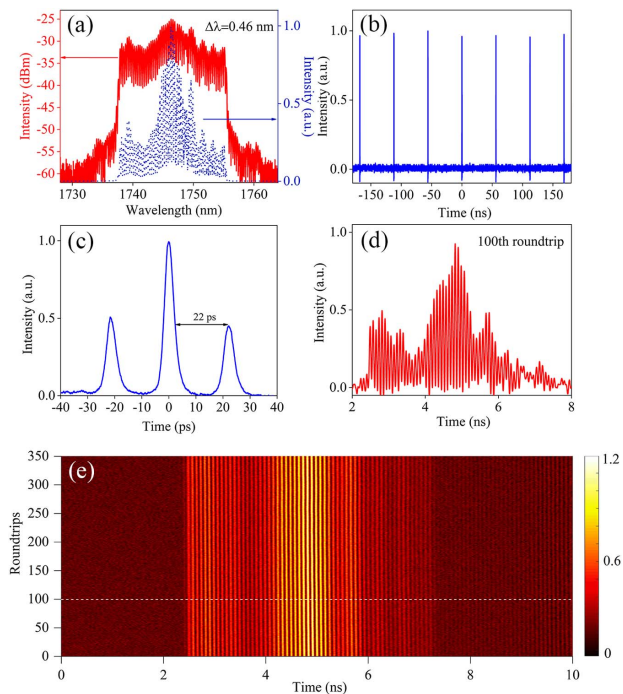


**Fig. 4.** Soliton molecule. (a) Spectrum; (b) pulse train; (c) autocorrelation trace; (d) single-shot spectrum of the 100th round trip; (e) shot-to-shot spectra of 350 round trips.

intensity modulation can be seen on the mode-locked spectrum, which is a typical characteristic of soliton molecules.

To further confirm the operation regime of the fiber laser, the autocorrelation trace was measured to check the fine details of the pulse profile, as shown in Fig. 4(c). Here, the autocorrelation trace indicated that the soliton molecule consists of two solitons with 22 ps separation, where their intensities are almost the same. Note that the 22 ps temporal separation is consistent with the 0.46 nm spectral modulation period. To investigate the phase stability between two solitons inside the molecule, we recorded the shot-to-shot interference pattern of the mode-locked spectrum by the DFT technique and plotted it in Fig. 4(e). It can be seen that the interference pattern of the soliton molecule is almost the same versus propagation round trips, demonstrating that the soliton molecule is stable without any evolving phase relationship of two solitons [36,37]. In addition, the single-shot spectrum at the 100th round trip is presented in Fig. 4(d), which also exhibits the evident interference pattern.

For a fiber laser, the mode-locked soliton will operate in a chaotic multi-pulse regime at a high pump power level, namely noise-like pulse [38]. Therefore, when the pump power was further increased to 1.3 W, the dissipative soliton evolved into the noise-like pulse regime. Figure 5(a) is the corresponding optical spectrum of the noise-like pulse, where the center wavelength and 3-dB spectral bandwidth are 1746 nm and 16 nm, respectively. The mode-locked spectrum shows the typical characteristics of the noise-like pulse, such as broad bandwidth and Gaussian profile. Essentially, the noise-like pulse is a wave packet that consists of numerous ultrashort pulses with

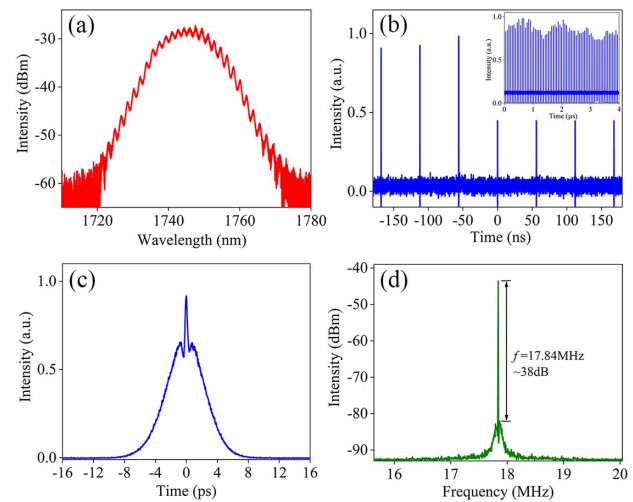


**Fig. 5.** Noise-like pulse. (a) Spectrum; (b) pulse train; inset: pulse train over 4  $\mu$ s; (c) autocorrelation trace; (d) RF spectrum.

randomly varying amplitude and phase among them. Therefore, being different from the mode-locked soliton, the noise-like pulse train exhibits evident intensity fluctuations, as shown in Fig. 5(b). The autocorrelation trace in Fig. 5(c) shows a narrow coherent peak with broad shoulders, which is a typical feature of the noise-like pulse. Moreover, the corresponding RF spectrum further demonstrated that the fiber laser operated in the noise-like pulse regime, in which there is a pedestal on it, as depicted in Fig. 5(d).

As we all know, generally a broader bandwidth of the mode-locked spectrum will lead to a shorter pulse duration according to the time-bandwidth product theory. In addition, the bandwidth of the mode-locked spectrum has been demonstrated to be related to the net cavity dispersion value, where the near-zero net-normal dispersion favors the generation of the broadband mode-locked soliton [29]. Thus, we were able to push the pulse duration (spectral bandwidth) to a shorter (broader) one by further engineering the cavity dispersion. To this end, the cavity net-normal dispersion of the fiber laser was gradually decreased by cutting the length of the UHNA4 fiber, while keeping the length of other fiber segments fixed. In this case, we could achieve the mode-locked dissipative soliton under different values of the net-normal cavity dispersion. Meanwhile, the output pulses were compressed separately outside the laser cavity by using different lengths of SMF. The typical mode-locked spectra with four cavity dispersion values were presented in Figs. 6(a)–6(d). It is expected that the spectral bandwidth broadens with the decreasing cavity dispersion. Note that the central wavelength of the dissipative soliton was shifted here, which is also due to the Lyot filtering effect in NPR mode-locked fiber laser [30]. Figures 6(e)–6(h) show the four de-chirped pulse autocorrelation traces corresponding to mode-locking states in Figs. 6(a)–6(d). In our experiment, the broadest spectrum ranging from  $\sim 1720$  nm to  $\sim 1770$  nm could be achieved when the net cavity dispersion was adjusted to be  $0.08 \text{ ps}^2$ . Correspondingly, the shortest de-chirped pulse duration is 230 fs. The pulse energy of 230 fs

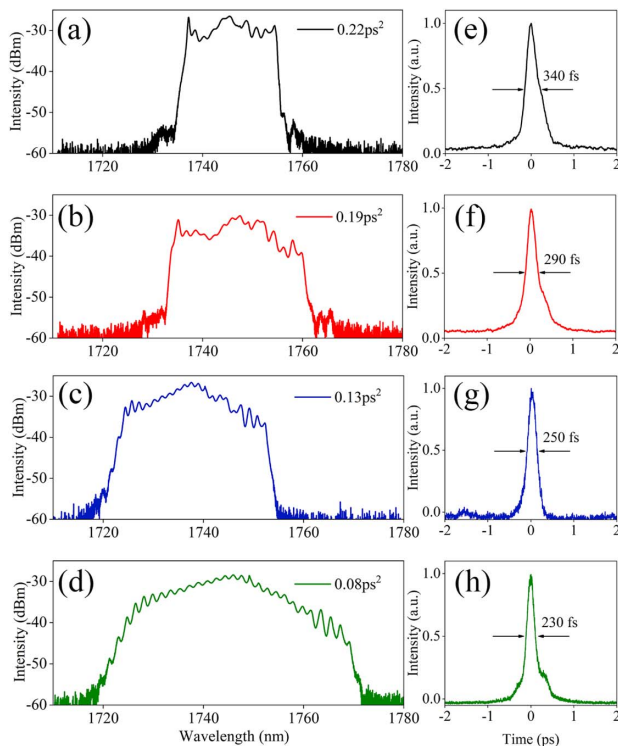


**Fig. 6.** (a)–(d) Mode-locked spectra with different net-cavity GDD; (e)–(h) corresponding autocorrelation traces.

dissipative soliton was measured to be  $\sim 0.2$  nJ. The time-bandwidth product is 0.497 for 230 fs pulse, indicating that the mode-locked soliton is almost transform-limited. Note that the pedestal on the autocorrelation trace in Fig. 6 may be caused by the nonlinear phase accumulation in the SMF for pulse compression.

#### 4. DISCUSSION

It is important to note that the spectra we measured have some periodic modulation peaks. These modulation peaks are different from the periodic spectral fringes formed by the interference of two pulses in the soliton molecule. To understand the reason for this modulation peak, we tried to change the position of components in the cavity. Then, we find that those periodic modulation peaks are more obvious in the spectra when the UHNA4 fiber is located after the TDF gain fiber. In fact, when the fundamental mode from the SMF couples into the UHNA4 fiber, higher-order modes can be excited due to the core diameter mismatching between the UHNA4 fiber (core diameter  $2.2\text{ }\mu\text{m}$ ) and the SMF (core diameter  $8.2\text{ }\mu\text{m}$ ). When these excited modes with different effective refractive indices are recoupled into the SMF, they will interfere with each other if the interference condition is satisfied, resulting in a spectral filtering effect [39]. Note that the pulse is amplified to a higher power after the TDF. Thus, these excited modes can be transmitted over long distances and then coupled into the next segment of SMF. However, if the UHNA4 fiber is placed at other cavity positions, these excited modes cannot

transmit over a long distance of UHNA4 fiber. This is why the modulation pattern is most pronounced when the UHNA4 fiber is located after the TDF gain fiber. In the experiment, the energy of the dissipative soliton was mostly limited by the wave-breaking effect. It should be also noted that the UHNA4 fiber with a smaller core diameter results in a higher nonlinear coefficient. In this case, a larger nonlinear phase shift is experienced by the dissipative soliton when passing through the UHNA4 fiber. With excessive nonlinear phase, the pulse chirp becomes nonmonotonic, leading to optical wave breakup and limiting the energy of the output dissipative soliton in our current setup [40].

It is also known that TDFs exhibit strong quasi-three-level system behavior in the shortwave emission region, which is characterized by the high pump power required and the reabsorption effect. For gain fiber with high dopant concentration, the reabsorption phenomenon is even more pronounced. Therefore, a relatively low dopant concentration gain fiber was chosen in our work. In addition, due to the low emission cross section and strong reabsorption effect of the gain fiber at the  $1.7\text{-}\mu\text{m}$  wave band, the length of the gain fiber has a significant impact on the  $1.7\text{-}\mu\text{m}$  gain. Thus, the dopant concentration and length of the gain fiber need to be carefully chosen to achieve better performance for  $1.7\text{-}\mu\text{m}$  dissipative soliton lasers [14,41]. In fact, specially fabricated normal dispersion TDF [18] has been reported recently. This makes the proposed  $1.7\text{-}\mu\text{m}$  dissipative soliton fiber laser ideal as a seed source for CPA systems to further obtain high-energy pulses in the  $1.7\text{-}\mu\text{m}$  wave band.

#### 5. CONCLUSION

In conclusion, we have experimentally demonstrated the  $1.7\text{-}\mu\text{m}$  dissipative solitons from a mode-locked Tm-doped fiber laser. Thanks to UHNA4 fiber, we were able to achieve net-normal dispersion of the cavity and force the laser to operate in the dissipative soliton regime. The fiber oscillator delivered the dissipative soliton with a pulse duration of 3.9 ps, which could be further compressed to 370 fs. By increasing the pump power and adjusting the PC, multi-pulse patterns such as soliton molecules and noise-like pulses were also observed. After optimizing the cavity dispersion by reducing the length of UHNA4 fiber, the dissipative soliton with 50 nm spectral width and de-chirped 230 fs pulse duration was obtained. The experimental results would pave the way for further investigations of high-energy pulse generation at the  $1.7\text{-}\mu\text{m}$  wave band, which might be useful to the communities dealing with the laser technology and the related application fields such as biomedical imaging.

**Funding.** Key-Area Research and Development Program of Guangdong Province (2018B090904003, 2020B090922006); National Natural Science Foundation of China (11874018, 11974006, 61805084, 61875058); Science and Technology Program of Guangzhou (2019050001); Guangdong Basic and Applied Basic Research Foundation (2019A1515010879).

**Disclosures.** The authors declare no conflicts of interest.

## REFERENCES

1. M. E. Fermann and I. Hartl, "Ultrafast fibre lasers," *Nat. Photonics* **7**, 868–874 (2013).
2. C. Kerse, H. Kalaycıoğlu, P. Elahi, B. Çetin, D. K. Kesim, Ö. Akçaalan, S. Yavaş, M. D. Aşık, B. Öktem, H. Hoogland, R. Holzwarth, and F. Ö. Ilday, "Ablation-cooled material removal with ultrafast bursts of pulses," *Nature* **537**, 84–88 (2016).
3. N. G. Horton, K. Wang, D. Kobat, C. G. Clark, F. W. Wise, C. B. Schaffer, and C. Xu, "In vivo three-photon microscopy of subcortical structures within an intact mouse brain," *Nat. Photonics* **7**, 205–209 (2013).
4. E. Agrell, M. Karlsson, A. R. Chraplyvy, D. J. Richardson, P. M. Krummrich, P. Winzer, K. Roberts, J. K. Fischer, S. J. Savory, B. J. Eggleton, M. Secondini, F. R. Kschischang, A. Lord, J. Prat, I. Tomkos, J. E. Bowers, S. Srinivasan, M. Brandt-Pearce, and N. Gisin, "Roadmap of optical communications," *J. Opt.* **18**, 063002 (2016).
5. S. P. Chong, C. W. Merkle, D. F. Cooke, T. Zhang, H. Radhakrishnan, L. Krubitzer, and V. J. Srinivasan, "Noninvasive, in vivo imaging of subcortical mouse brain regions with 1.7  $\mu\text{m}$  optical coherence tomography," *Opt. Lett.* **40**, 4911–4914 (2015).
6. M. Yamanaka, T. Teranishi, H. Kawagoe, and N. Nishizawa, "Optical coherence microscopy in 1700 nm spectral band for high-resolution label-free deep-tissue imaging," *Sci. Rep.* **6**, 31715 (2016).
7. C. Li, J. Shi, X. Gong, C. Kong, Z. C. Luo, L. Song, and K. K. Y. Wong, "1.7  $\mu\text{m}$  wavelength tunable gain-switched fiber laser and its application to spectroscopic photoacoustic imaging," *Opt. Lett.* **43**, 5849–5852 (2018).
8. K. Wang and C. Xu, "Tunable high-energy soliton pulse generation from a large-mode-area fiber and its application to third harmonic generation microscopy," *Appl. Phys. Lett.* **99**, 071112 (2011).
9. H. Y. Chung, W. Liu, Q. Cao, F. X. Kärtner, and G. Chang, "Er-fiber laser enabled, energy scalable femtosecond source tunable from 1.3 to 1.7  $\mu\text{m}$ ," *Opt. Express* **25**, 15760–15771 (2017).
10. S. Firstov, S. Alyshev, M. Melkumov, K. Riumkin, A. Shubin, and E. Dianov, "Bismuth-doped optical fibers and fiber lasers for a spectral region of 1600–1800 nm," *Opt. Lett.* **39**, 6927–6930 (2014).
11. S. D. Agger and J. H. Povlsen, "Emission and absorption cross section of thulium doped silica fibers," *Opt. Express* **14**, 50–57 (2006).
12. S. D. Jackson, "The spectroscopic and energy transfer characteristics of the rare earth ions used for silicate glass fibre lasers operating in the shortwave infrared," *Laser Photonics Rev.* **3**, 466–482 (2009).
13. Z. Li, Y. Jung, J. M. O. Daniel, N. Simakov, M. Tokurakawa, P. C. Shardlow, D. Jain, J. K. Sahu, A. M. Heidt, W. A. Clarkson, S. U. Alam, and D. J. Richardson, "Exploiting the short wavelength gain of silica-based thulium-doped fiber amplifiers," *Opt. Lett.* **41**, 2197–2200 (2016).
14. L. Zhang, J. Zhang, Q. Sheng, S. Sun, C. Shi, S. Fu, X. Bai, Q. Fang, W. Shi, and J. Yao, "Efficient multi-watt 1720 nm ring-cavity Tm-doped fiber laser," *Opt. Express* **28**, 37910–37918 (2020).
15. C. Li, X. Wei, C. Kong, S. Tan, N. Chen, J. Kang, and K. K. Y. Wong, "Fiber chirped pulse amplification of a short wavelength mode-locked thulium-doped fiber laser," *APL Photonics* **2**, 121302 (2017).
16. T. Noronen, O. Okhotnikov, and R. Gumenyuk, "Electronically tunable thulium-holmium mode-locked fiber laser for the 1700–1800 nm wavelength band," *Opt. Express* **24**, 14703–14708 (2016).
17. C. Li, C. Kong, and K. K. Y. Wong, "High energy noise-like pulse generation from a mode-locked thulium-doped fiber laser at 1.7  $\mu\text{m}$ ," *IEEE Photonics J.* **11**, 1505106 (2019).
18. S. Chen, Y. Chen, K. Liu, R. Sidharthan, H. Li, C. J. Chang, Q. J. Wang, D. Tang, and S. Yoo, "All-fiber short-wavelength tunable mode-locked fiber laser using normal dispersion thulium-doped fiber," *Opt. Express* **28**, 17570–17580 (2020).
19. D. Anderson, M. Desaix, M. Lisak, and M. L. Quiroga-Teixeiro, "Wave breaking in nonlinear-optical fibers," *J. Opt. Soc. Am. B* **9**, 1358–1361 (1992).
20. A. Chong, W. H. Renninger, and F. W. Wise, "All-normal-dispersion femtosecond fiber laser with pulse energy above 20 nJ," *Opt. Lett.* **32**, 2408–2410 (2007).
21. P. Grelu and N. Akhmediev, "Dissipative solitons for mode-locked lasers," *Nat. Photonics* **6**, 84–92 (2012).
22. D. Strickland and G. Mourou, "Compression of amplified chirped optical pulses," *Opt. Commun.* **56**, 219–221 (1985).
23. T. Eidam, S. Hanf, E. Seise, T. V. Andersen, T. Gabler, C. Wirth, T. Schreiber, J. Limpert, and A. Tünnermann, "Femtosecond fiber CPA system emitting 830 W average output power," *Opt. Lett.* **35**, 94–96 (2010).
24. D. Luo, Y. Liu, C. Gu, Z. Zhu, Z. Deng, L. Zhou, Y. Di, G. Xie, and W. Li, "130 W, 180 fs ultrafast Yb-doped fiber frequency comb based on chirped-pulse fiber amplification," *Opt. Express* **28**, 4817–4824 (2020).
25. B. J. Ainslie and C. R. Day, "A review of single-mode fibers with modified dispersion characteristics," *J. Lightwave Technol.* **4**, 967–979 (1986).
26. Q. Wang, T. Chen, M. Li, B. Zhang, Y. Lu, and K. P. Chen, "All-fiber ultrafast thulium-doped fiber ring laser with dissipative soliton and noise-like output in normal dispersion by single-wall carbon nanotubes," *Appl. Phys. Lett.* **103**, 011103 (2013).
27. B. G. Bale, J. N. Kutz, A. Chong, W. H. Renninger, and F. W. Wise, "Spectral filtering for high-energy mode-locking in normal dispersion fiber lasers," *J. Opt. Soc. Am. B* **25**, 1763–1770 (2008).
28. P. Ciąćka, A. Rampur, A. Heidt, T. Feurer, and M. Klimczak, "Dispersion measurement of ultra-high numerical aperture fibers covering thulium, holmium, and erbium emission wavelengths," *J. Opt. Soc. Am. B* **35**, 1301–1307 (2018).
29. L. E. Nelson, D. J. Jones, K. Tamura, H. A. Haus, and E. P. Ippen, "Ultrashort-pulse fiber ring lasers," *Appl. Phys. B* **65**, 277–294 (1997).
30. W. S. Man, H. Y. Tam, M. S. Demokan, P. K. A. Wai, and D. Y. Tang, "Mechanism of intrinsic wavelength tuning and sideband asymmetry in a passively mode-locked soliton fiber ring laser," *J. Opt. Soc. Am. B* **17**, 28–33 (2000).
31. Y. C. Tong, L. Y. Chan, and H. K. Tsang, "Fibre dispersion or pulse spectrum measurement using a sampling oscilloscope," *Electron. Lett.* **33**, 983–985 (1997).
32. K. Goda and B. Jalali, "Dispersive Fourier transformation for fast continuous single-shot measurements," *Nat. Photonics* **7**, 102–112 (2013).
33. D. Y. Tang, L. M. Zhao, B. Zhao, and A. Q. Liu, "Mechanism of multi-soliton formation and soliton energy quantization in passively mode-locked fiber lasers," *Phys. Rev. A* **72**, 043816 (2005).
34. S. S. Xu, M. Liu, Z. W. Wei, A. P. Luo, W. C. Xu, and Z. C. Luo, "Multipulse dynamics in a Mamyshev oscillator," *Opt. Lett.* **45**, 2620–2623 (2020).
35. X. Liu and M. Pang, "Revealing the buildup dynamics of harmonic mode-locking states in ultrafast lasers," *Laser Photonics Rev.* **13**, 1800333 (2019).
36. A. Zavyalov, R. Iliev, O. Egorov, and F. Lederer, "Dissipative soliton molecules with independently evolving or flipping phases in mode-locked fiber lasers," *Phys. Rev. A* **80**, 043829 (2009).
37. K. Krupa, K. Nithyanandan, U. Andral, P. Tchofo-Dinda, and P. Grelu, "Real-time observation of internal motion within ultrafast dissipative optical soliton molecules," *Phys. Rev. Lett.* **118**, 243901 (2017).
38. M. Horowitz, Y. Barad, and Y. Silberberg, "Noiselike pulses with a broadband spectrum generated from an erbium-doped fiber laser," *Opt. Lett.* **22**, 799–801 (1997).
39. B. Dong, L. Wei, and D. P. Zhou, "Coupling between the small-core-diameter dispersion compensation fiber and single-mode fiber and its applications in fiber lasers," *J. Lightwave Technol.* **28**, 1363–1367 (2010).
40. W. H. Renninger, A. Chong, and F. W. Wise, "Area theorem and energy quantization for dissipative optical solitons," *J. Opt. Soc. Am. B* **27**, 1978–1982 (2010).
41. M. D. Burns, P. C. Shardlow, P. Barua, T. L. Jefferson-Brain, J. K. Sahu, and W. A. Clarkson, "47 W continuous-wave 1726 nm thulium fiber laser core-pumped by an erbium fiber laser," *Opt. Lett.* **44**, 5230–5233 (2019).